

Anomalous inter-layer atomic transport and the low-temperature amplification of surface instability in Al(111)

P. Süle

*Research Institute for Technical Physics and Material Science,
Konkoly Thege u. 29-33, Budapest, Hungary, sule@mfa.kfki.hu, www.mfa.kfki.hu/~sule,
(April 27, 2017)*

Anomalous inter-layer atomic transport of deposited impurity atoms on Al(111) has been found by constant temperature molecular dynamics simulations. The low-energy deposition of Pt on Al(111) leads to oscillatory adsorbate-substrate interaction and to a low-temperature ballistic injection of the deposited particles to below the topmost layer. The ultrafast injection of a Pt atom coincides with the ejection of a substrate atom to the surface (ballistic replacement or exchange mechanism). This is in agreement with the experimental findings in which thin film rich in Al has been found on the surface after deposition of few MLs of Pt. We attribute the anomalous inter-layer transport to the size-mismatched impurity/host interaction and we point out the role of atomic size mismatch in biasing towards intermixing. The deposition induced low-temperature disordering of surface Al atoms with few transient Al adatoms has also been observed. The ultrafast injection of the impurity particles to the substrate is assisted by the transient out-of-plane and lateral circulating motion of few surface atoms arranged nearly in a hexagonal symmetry. The atomic injection of Pt can be regarded as a superexchange process driven by the transient and collective motion of few surface atoms. A chaotic surface state assisted mechanism could also be a possible explanation of the unexpected phenomenon.

PACS numbers: 68.43.Jk, 68.35.Fx, 66.30.-h

Keywords: interdiffusion, atomic size-mismatch, athermal mixing, particle impact, chaotic transport, anomalous diffusion, superdiffusion, local acceleration, vapor deposition, intermixing

I. INTRODUCTION

The understanding of the fundamental atomistic transport processes leading to the formation and morphological evolution of nanoscale surface features is lacking [1]. Many classical macroscopic (continuum and mesoscopic) models for diffusion and morphological evolution lose their validity in the nanoscale [1,2]. Therefore the atomistic level understanding of the driving forces and mechanisms governing atomic transport involved in the synthesis and organisation of nanoscale features in solid state materials including atomic intermixing, is inevitable [1].

The most well known atomic diffusion mechanisms of adatoms on solid surfaces are the hopping diffusion on the surface from one site to another over a bridge site and the atomic site exchange when an adatom enters the topmost layer and a surface atom becomes an adatom [3]. The atoms deposited at surfaces could undergo, however, few exotic (or anomalous) transport processes such as random walk or Levy flight [3–5], Friedel-type adsorbate-adsorbate oscillatory interaction driven relaxations [3,6–9], intermixing and surface alloying between immiscible elements [7,10,11,14], long range surface mediated lateral mass transport within the topmost layer [12] and very fast kinetics with low diffusion barrier driven by quantum size effects [13]. The low-energy ion-bombardment induced ejection of Al atoms to the Al(111) surface results in adatoms with ultrafast motion on the surface leading to the formation of nanodots [15]. These atomic migrations can be characterized by the lateral transport of atoms on the surface or within

the topmost layer. Inter-layer transport occurs only between the surface and the topmost layer or at step edges, however, the most of these processes can not usually be considered as anomalous, e.g. the rate of the process can be described within the framework of the Arrhenius equation. Anomalous atomic processes are athermal and the mean free path of the atomic jumps can reach the few times of the nearest neighbor distance [3,4]. Also, the mean square of atomic displacements scales nonlinearly in the course of time of diffusion [4,16] or the nanoscale growth rate of interfaces follows linear growth kinetics (nonparabolic growth) [2].

However, only few examples are known for inter-layer mass transport (atomic jumps normal to the surface) which can be considered as anomalous. Even in these articles the authors not always realized the anomalous nature of inter-layer transport. The assistance of instantaneously high kinetic energy to inter-layer transport during the deposition of Au on Ag surface has been reported [17]. Interdiffusive Stranski-Krastanov growth mode in an analysis of scanning tunneling microscopy data and the burrowing of Au particles in Ag(110) when annealing has been applied during simulations (replacement diffusion mechanism) have also been found [18]. In another study a complicated exchange mechanism is shown with ballistically injected deposited Au on Ag(111) [19]. Sprague et al. has been published interface mixing on impact (athermal mixing) for the case of Pt deposition on Cu and which is explained by the attractive potentials of the substrate atoms and a large thermodynamic bias toward film-substrate mixing [20]. The mechanism of

the seemingly different transient atomic migrations could hopefully be explained in a common framework.

The understanding of how adsorbed impurities and growing film constituents affect interdiffusion to the substrate needs further studies of the atomistic mechanism of intermixing. For instance, using vapor deposition of various transition metals on Al, it has been found that the intermixing (IM) length is anomalously large in certain cases [21]. It has also been characterized that IM is not driven by bulk diffusion parameters [21] nor by bulk thermochemistry (such as heats of alloying) during ion-beam mixing [22,23]. The segregation of Al during vapor deposition of Pt on polycrystalline Al together with the fast reactive diffusion of Pt to the bulk have also been found [21,24]. In another study the adsorption of Pt on polycrystalline Al leads to the formation of surface alloys [25] which are rich in Al [26].

Anharmonic effects, surface disordering and premelting has also been studied intensively at fcc (111) metal surfaces [27,28]. It has also been concluded that surface thermal expansion and lattice dynamics might be anomalous of the (111) surface layer of Al [27,36] hence Al can be described by unusual surface instability. It would be interesting if e.g. the surface of Al would be subjected to small external perturbation such as the deposition of an impurity atom. Owing to the anharmonic surface behavior of Al(111) the amplification of surface instability could be expected.

A number of unconventional atomic transport phenomena have been explained by atomic size-mismatch (ASM) of the constituents [10,16,29–35]. Surface alloying and intermixing between many immiscible and even miscible elements can not solely be explained by thermodynamic and chemical forces such as heat of alloying and mixing or cohesive energies [10,11,14,22,23]. The puzzling nature of intermixing (IM) might be due to still an unknown and an unconventional mechanism which has not been explored yet or overlooked in the last decades. In our previous reports we explained IM as an interfacial anisotropy driven process in diffusion couples and pointed out the role of mass and size-anisotropy during ion-bombardment induced interdiffusion [15,16,22].

In the present article, we show that anomalous atomic transport occurs during vapor deposition in size-mismatched systems, such as during the thin film growth of Pt and other transition metals on Al(111). The interdiffusion of the deposited particle is driven by an oscillatory interaction with the surface atoms of the substrate. Moreover, we point out that the anomalous character of the atomic transport of the deposit can be tuned by adjusting the ASM of the constituents. We present an exchange mechanism with a concerted motion of few surface atoms for entering the uppermost layer by the deposited particle. Also, we show that large atomic vibrational displacements and anharmonic effects might occur not only at high-temperatures close to the melting point, but also at ultra-low temperatures induced by impurities at the surface.

II. THE SIMULATION METHOD

A. General properties

We give the detailed outline of the employed simulation approach. Classical constant volume tight-binding molecular dynamics simulations [43] were used to simulate soft landing and vapor deposition of Pt atoms on Al(111) and also on other substrates (such as Cu(111)) surface at ~ 0 K using the PARCAS code [37]. The PARCAS MD code has widely been used for the study of various atomic transport phenomena in the last few years [22,38]. A variable timestep and the Berendsen temperature control is used [39,40]. The simulation uses the Gear’s predictor-corrector algorithm to calculate atomic trajectories [39]. The maximum time step of 0.05 fs is used. We consider the coupling of our simulation cell to a heat bath by inserting stochastic and friction terms to the equation of motion yielding a Langevin type equation (see details in refs. [39–41]). The equation of motion can be written as follows,

$$m_i \dot{v}_i = \mathbf{F}_i - m_i \gamma_i v_i + R(t), \quad (1)$$

where \mathbf{F}_i is the force on atom i and $R(t)$ is a Gaussian stochastic variable. The damping constants γ_i determine the strength of coupling to the thermostat. The global coupling to the heat bath can be adjusted by the so called Berendsen temperature which we set to 70 K. The system couples to a heat bath not only globally via the damping constant but is also locally subjected to random noise. Stochastic forces and damping applied at the cell borders (lateral $x - y$ boundaries as heat sink) of the simulation cell to maintain constant temperature conditions and the thermal equilibrium of the entire system (coupling to the heat bath). The top of the simulation cell is left free (the free surface) for the deposition of Pt atoms. The bottom layers are held fixed in order to avoid the rotation of the cell. system. For simulating deposition it is appropriate to use temperature control at the cell borders. This is because it is physically correct that potential energy becomes kinetic energy on impact, i.e. heats the lattice. This heating should be allowed to dissipate naturally, which means temperature control should not be used at the impact point. Periodic boundary conditions are imposed laterarily. The observed anomalous transport processes are also observed without periodic boundary conditions and temperature control. Further details are given in [37] and details specific to the current system in recent communications [22,23].

The size of the simulation cell is $80 \times 80 \times 42 \text{ \AA}^3$ including 16128 atoms (with a fcc lattice). 15 active MLs are supported on 3 fixed bottom monolayers (MLs). We find no dependence of the anomalous atomic transport properties of the deposited atoms on the finite size of the simulation cell. Deposited atoms were initialized normal to the (111) surface with randomly selected lateral positions 4 – 5 \AA above the surface.

The kinetic energy of the deposited particles are ~ 0.1 eV or in the case of ultrasoft landing it is nearly zero eV. The impurity (deposited) particle is placed $4 - 5 \text{ \AA}$ above the (111) surface of the substrate. No acceleration of the deposited particle is observed above 6 \AA the surface. We also analyze the acceleration of the deposited particles and calculate the arrival energy at the surface of the substrate. Using the history (movie) file we collect the atomic positions of the moving substrate atoms which have kinetic energy above a certain threshold value in order to get the pattern of atomic trajectories during the deposition events. At 0 K this value is ~ 0.01 eV. In order to make a statistics of impact events we generated 100 events with randomly varied impact positions.

In order to follow the time evolution of atomic motions the mean square of the atomic displacements $\langle R^2 \rangle$ (MSD) has been calculated. $\langle R^2 \rangle = \sum_i^N [\mathbf{r}_i(t) - \mathbf{r}_i(t=0)]^2$, as obtained by molecular dynamics simulations and ($\mathbf{r}_i(t)$ is the position vector of atom 'i' at time t) and N is the number of atoms included in the sum, respectively. We also calculate $\langle R^2 \rangle$ for the impurity atom only, hence in this case $\langle R^2 \rangle = (\mathbf{r}_i(t) - \mathbf{r}_i(t=0))^2$. In other cases lateral or vertical (out-of-plane) components are included in $\langle R^2 \rangle$ for the substrate atoms. We follow the evolution of $\langle R^2 \rangle$ during few events in order to get a reasonable statistics of atomic motions.

B. The interaction potentials

We use the many-body Cleri-Rosato (CR) tight-binding second-moment approximation (TB-SMA) interaction potential to describe interatomic interactions [43]. The CR potential is formally analogous to the embedded atomic method (EAM, [52]) formalism, e.g. the potential energy of an atom is given as a sum of repulsive pair potentials for the neighboring atoms (usually for the first or second neighbors and a cutoff is imposed out of this region) and an embedding energy that is a function of the local electron density given as follows [52],

$$E_{tot} = \frac{1}{2} \sum_{ij} V(r_{ij}) + \sum_i F[\rho_i], \quad (2)$$

where r_{ij} is the distance between atoms i and j and its neighbors. There are many functional forms are available for the density ρ_i and for the embedding function $F[\rho_i]$ [52]. We utilize EAM functional forms in the code for $F[\rho_i]$ and for the density ρ similar to that given in refs. [52,53]. The EAM routine in the code employs a cubic spline interpolation for the evaluation of the EAM potentials and their derivatives (forces) starting from various kind of input potentials given in discrete points as a function of r_{ij} (the number of points per functions is 5000 in this study).

Within the second moment tight-binding approach, the band energy (the attractive part of the potential) reads,

$$E_b^i = - \left[\sum_{j, r_{ij} < r_c} \xi^2 \exp \left[-2q \left(\frac{r_{ij}}{r_0} - 1 \right) \right] \right]^{1/2}, \quad (3)$$

where r_c is the cutoff radius of the interaction and r_0 is the first neighbor distance (atomic size parameter).

The repulsive term is a Born-Mayer type phenomenological core-repulsion term:

$$E_r^i = A \sum_{j, r_{ij} < r_c} \exp \left[-p \left(\frac{r_{ij}}{r_0} - 1 \right) \right]. \quad (4)$$

The parameters (ξ, q, A, p, r_0) are fitted to experimental values of the cohesive energy, the lattice parameter, the bulk modulus and the elastic constants c_{11} , c_{12} and c_{44} [43]. The summation over j is extended up to fifth neighbors for fcc structures [43]. The total cohesive energy of the system is

$$\begin{aligned} E_c &= - \sum_{i, j, r_{ij} < r_c, i \neq j} \int_0^\infty \frac{\partial U(\mathbf{r})}{\partial \mathbf{r}} \bigg|_{r=r_{ij}} \frac{\overline{r_{ij}}}{r_{ij}} d\mathbf{r} \\ &= \sum_i (E_r^i + E_b^i), \end{aligned} \quad (5)$$

where $U(\mathbf{r})$ is the total potential energy of the entire system as a function of the space coordinate (radius vector) \mathbf{r} since the system is energy conservative, the space integral over the Newtonian interatomic forces gives the total energy of the simulation cell. \mathbf{r} can be replaced by the internuclear separation r_{ij} in the pair interaction term $V(r_{ij})$ and by the position vector of the electron density in the density function $\rho_i(r)$ in Eq. (2). Formally we give all the terms in Eqs. (3)-(4) in the same way as for EAM potentials except that $F[\rho_i]$ is calculated in a tight-binding form as given in Eq. (3). We prefer to use the CR potential because r_0 can be tuned in this case which is proportional to the atomic size-mismatch in the heteronuclear potential (the proportionality will be discussed later in section III.). Using the CR potential we consider the interaction between two atoms and the interaction with their local environment usually up to the second neighbors. Out of this region a potential cutoff is imposed. The cutoff radius r_c is taken as the second neighbor distance for all the interactions. We tested the Al-Al and the Al-Pt potential at cutoff radius with third and larger neighbor distances and found no considerable change in the results. The CR potential gives the physically reasonable representation of metals and computationally is efficient hence nanoscale atomic clusters with large number of atoms (up to millions of atoms) can be simulated. This type of a potential gives a very good description of lattice vacancies, including migration properties and a reasonable description of solid surfaces and melting [43]. Since the present work is mostly associated with the elastic properties, melting behaviors, surface, interface and migration energies, we believe the model used should be suitable for this study. In a recent report we found that the CR potential describes properly Al and

Al/Pt [15] and provides reasonable results for the ion-bombardment of Al(111) in agreement with the experimental results [3]. The CR potential correctly provides the adatom binding and dimerization energies, adatom island formation upon ion-bombardment in agreement with experiment [56]. Recently it has also been shown, that the CR potential remarkably well describes diffusion in liquid Al [45,46] and energetic deposition of Al clusters on Al [47]. In order to be more convincing in the accuracy of the TB-SMA model we also used another parameterization set for Eqs. (3)-(4) obtained by first principles augmented-plane-wave calculations [44]. This parameterization offers a satisfactory agreement with the experimental data for thermal expansion coefficient, the temperature dependence of the atomic mean-square of displacement and the phonon density of states of compounds [44]. However, we find no serious difference in the final results obtained for deposition between the CR and the parameterization of Papanicolau *et al.*. Therefore we use the original CR parameterization set for Al.

Despite the empirical nature of the EAM and CR potentials their accuracy seems to be sufficient for studying materials under nonequilibrium conditions such as anharmonic effects and thermal expansion of various fcc metals [27,28]. In the present paper we use these potentials for the investigation of low-temperature disordering processes with transient surface atomic vibrations for which the EAM and CR potentials should be adequate [27,15].

For the crosspotential of substrate atoms and Pt we employ an interpolation scheme [15,22,48] using the geometrical mean of the elemental energy constants and the harmonic mean for the screening length of Eqs. (3)-(4) are taken as in refs. [48,49]. The CR elemental potentials and the interpolation scheme for heteronuclear interactions have widely been used for MD simulations [11,14,22,31,50]. Recently CR interpolated crosspotential has also successfully been used for Ti/Pt in agreement with our experimental results [16]. The scaling factor r_0 (the heteronuclear first neighbor distance) is calculated as the average of the elemental first neighbor distances. The AlPt potential is fitted to the measured effective heat of mixing in the cubic AlPt ($\Delta H \approx -100$ kJ/mol) with a melting temperature of 1870 K [51] which is reproduced by our Cleri-Rosato crosspotential within the range of 1800 ± 100 K. In order to adjust ΔH in the AlPt potential (which is proportional to the strength of the interaction and to the heat of alloying in the AlPt alloy) the preexponential parameter ξ in Eq (3) is set to $\xi \approx 3.0$ [15]. Adjusting ξ in Eq (3) one can tune the depth of the crosspotential well which is proportional to ΔH [15,23].

We find, however, that the interdiffusive features of Pt in Al does not depend significantly on heat of mixing built in the potential in accordance with our earlier findings for ion-bombardment induced intermixing in Ti/Pt [23]. The injective (ballistic) mixing of Pt takes place on a broad range of ΔH values including purely repulsive crosspotential ($\Delta H = 0$, $\xi \approx 0$, attractive term given in Eq. (3) is cancelled). This is because anomalous diffusion

might not be driven by thermodynamic bias (athermal mixing) [22]. The real driving force of athermal (ballistic) mixing is far from being understood clearly yet [22,23].

Depositing Pt on Al(111) using Ercolesi-Adams (EA) Al-Al potential based on the embedded atomic method [52,54] we get also injection when the cross pair-potential is obtained by the Johnson's scheme [55] which reads as

$$V_{AB}(r) = \frac{1}{2} \left[\frac{\rho_B}{\rho_A} V_A(r) + \frac{\rho_A}{\rho_B} V_B(r) \right]. \quad (6)$$

Hence the heteronuclear pair potential is given as the function of the elemental potentials. To avoid singularities, cutoff must be imposed for the density functions ρ_A and ρ_B equal or greater than the cutoff distance for the $V_A(r)$ and $V_B(r)$ potentials. The cross-embedding function is given as the elemental average of $F[\rho_i]$ functions. The EA potential has been fitted to *ab initio* atomic forces of many different configurations using the force matching method [54]. Recently, it has been shown, that the EA potential correctly describes thermal expansion behavior [54] and anharmonic effects at Al surfaces [36,27]. Hence the transferability of the EAM potentials to nonequilibrium conditions of Al seems to be sufficient.

III. THE ATOMIC SIZE-MISMATCH CONCEPT

Since we study the dependence of atomic dynamics on ASM we briefly discuss our approach to ASM. To account for ASM the lattice mismatch (LM) concept has widely been used in the literature which is given as the ratio of the lattice constants of the film and substrate constituents [1,10,16,29-35]. In the present paper we use another quantity to describe size-mismatch in diffusion couples. The motivation for this is that LM seems not to explain interdiffusion and surface alloying in a number of binary systems [21]. Also, the observed asymmetry of intermixing in various metal film/substrate couples can not be understood within the LM concept [16,21]. In the LM concept it is assumed that intermixing and many other properties of binary systems (e.g. growth modes) are primarily determined by the ratio of atomic sizes (lattice constants) of the pure elemental phases. Instead we introduce the quantity atomic size mismatch (ASM) which is the ratio of the first neighbor distance r_0 of the deposited impurity in its alloy phase with the substrate ($r_0^{im,s}$, AlPt alloy in this case) to the r_0 of the substrate in its pure elemental phase (r_0^s). If no alloy exist between the constituents than $r_0^{im,s}$ is simply the average of the elemental r_0 values. Hence in the ASM concept the ratio $\delta_{ASM} = r_0^{im,s}/r_0^s$ depends on the cross-interaction between the impurity and substrate atoms. It is reasonable because the impurity atom when deposited on the substrate interacts directly with the substrate atoms hence mainly the heteronuclear interaction determines ASM at low impurity concentration and not its pure elemental

homonuclear r_0^{im} value. With increasing film thickness and film coverage the lattice constant of the film will be more and more important ingredient of the overall lattice misfit. In other words within this picture of ASM the atomic volume (size) is proportional to the local r_0 value which is strongly interaction and environment dependent. The same impurity can be described by different r_0 value in its pure and in an intermixed environment. In a strict sense the average $r_0 = (r_0^{im} + r_0^s)/2$ is the correct description of the heteronuclear first neighbor distance in the 1:1 alloy phases. In nonstoichiometric alloys or in inhomogeneous phases (such as intermixed nonequilibrium phases) $r_0^{im,s}$ fluctuates around the elemental average and locally $r_0^{im,s}$ can reach different values depending on the local stoichiometricity of the system. Nevertheless, the average r_0 seems to be a reasonable approximation for interfacial mixing [15,16].

In Pt/Al the magnitude of intermixing is not sensitive to the choice of r_0 for the deposition of Pt on Al within the range of [2.8; 3.0] Å, hence the elemental average of $r_0^{im,s} \approx 2.85$ Å is a reasonable choice. We prefer to use in most of the presented results the CR potential because the first neighbor distance r_0 can be tuned in the heteronuclear potential in this case which is proportional to ASM. Using EAM potentials such as given in Eq. (6) no effect of r_0 can be studied.

IV. RESULTS AND DISCUSSION

In the rest of the article we present results which seem to be rather surprising and unexpected. Since we find no reason on the methodological side to discard them (the employed simulation approach and the interaction potentials should be adequate for the problem) we feel it important to share these atomistic results with a wider community.

The simulation of vapor deposition leads to an unexpected result. The deposited atoms, independently of the energy of deposition, intermix with ultrafast atomic exchange entering the top Al(111) layer even at 0 K within a ps if initialized $< 4 - 5$ Å far from the surface. Also, the particle not only enter but becomes and interstitial atom between the two upper layers. The acceleration of the deposited particles have been found starting at ~ 5 Å distance from the surface. The injection of Pt goes together with the ejection of one Al atom to the surface. The deposition of 1 ML of Pt leads to the formation of an adlayer rich in Al in agreement with the experimental findings [21,24]. The ultrafast interdiffusion of Pt to Al is rather surprising, and similar superdiffusion during soft landing of atoms on solid surfaces has been reported only for Pt on Cu(111) [20]. The animation of the atomic injection can be seen in a web page [42]. The unexpected mechanism of Pt interdiffusion might not be an artifact of the CR potential. We have tested recently the various surface features of CR Al potential [15] and got fairly

nice results. Hence, we do not attribute the anomalous behavior of Pt soft landing on Al(111) to the artifact of the CR potential. We find direct injection only in the case of certain transition metal elements around Pt in the periodic table, such as Ir, Au. Other elements, such as Cu intermixes to Al after the deposition of dozens of atoms. Moreover, we do believe that the fast reactive interdiffusion reported in Pt/Al and in other diffusion couples must be due to anomalous diffusion which is overlooked in the literature. We get also a rapidly increasing intermixing length during the simulation of vapor deposition [42], although still we are far from the experimental value of ~ 50 Å [21] (results are not shown in this paper). We deposit few MLs of Pt which is insufficient to reach this value. In this article, however, it is not our intention to reproduce the experimental intermixing length. We rather focus on the understanding of the elementary atomic migration step of interdiffusion. We will examine in the rest of the paper the details of the mechanism of the ballistic interdiffusion of Pt.

Although we study the mechanism of an atomic jump, we discuss the details of an atomic transport step as a first step of the reactive diffusion to the bulk reported in many papers [21,24]. A number of such single atomic jumps leads to a diffusional process through the atomic layers of the substrate leading to the large intermixing length reported for Al [21]. We find the nonlinear (parabolic) scaling of $\langle R^2 \rangle$ as a function of time during interdiffusion which suggests that the atomic interlayer transport is anomalous [4]. An atomic transport is anomalous if the exponent $\alpha > 1$ or $\alpha < 1$ in the expression $\langle R^2 \rangle \propto t^\alpha$, where, t is the time variable [4].

We also vary the first neighbor distance r_0 in the heteronuclear potential, in order to point out the sensitivity of interdiffusion to ASM. The r_0 of the heteronuclear interaction is constructed as the average of the elemental values [22,48]. As we have already pointed out, the size-mismatch of the binary system is proportional to the ratio of $\delta_{ASM} = r_0^{AlPt}/r_0^{Al}$. In this particular case the Pt atom is the smaller particle ($r_0 \approx 2.8$) and $r_0 \approx 2.9$ in Al. Moreover Al has a highly anharmonic homonuclear interaction potential (see upper Fig 1). Due to the anharmonic behavior of Al there is a tendency for increased Al-Al distances ($r_0^{Al} \geq 2.9$) on the surface (see upper Fig 1). If we set $r_0 \approx 3.1$ Å, no injection is found (This is because $\delta_{ASM} \approx 1$). Ballistic atomic injection can be suppressed by tuning ASM. We also test deposition in other size-mismatched systems, such as Ni/Au. Injection occurs in this system, when unphysical values are used ($r_0 \leq 2.0$ Å).

In order to understand the details of the injective anomalous atomic transport the shape of the deposit-surface interaction energy potential is calculated. In lower Fig 1 we show the binding energy (potential energy) of the Pt atom as a function of the distance from the surface. An oscillatory impurity-substrate interaction potential is found. The amplitude of the oscillation is large (few eVs). The oscillation of the potential is

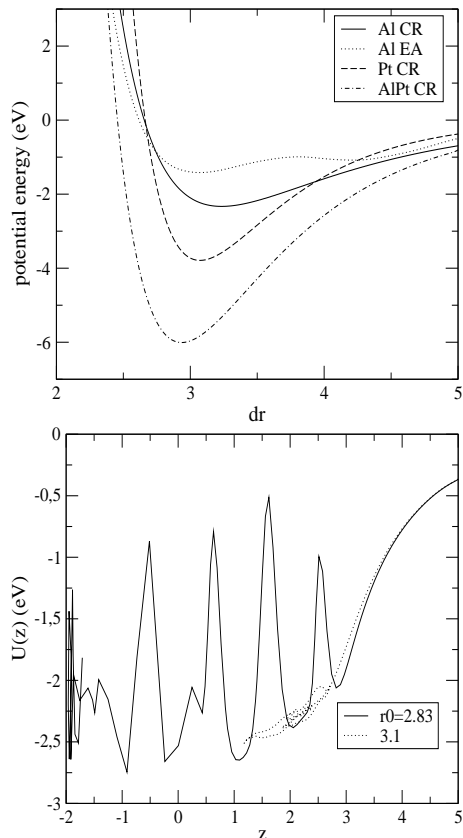


FIG. 1. *Upper panel:* The profiles of the potential energy as a function of the internuclear separation (r_{ij} , Å, for Al, Pt and for AlPt using the CR ($\xi = 3.0$ in Eq. (3)) and Ercolesi-Adams EAM (EA) potentials (Al only). *Lower panel:* The oscillatory potential energy profile of Pt (straight line) as a function of the distance (z) of the Pt atoms from the surface of Al(111) (the position of the surface is at 0 Å, $r_0 \approx 2.83$ Å). The potential (binding) energy of Pt with $r_0 \approx 3.1$ Å is given with a dotted line.

caused by the transient out-of-plane movements of surface Al atoms. We see also the reflection of the captured Pt atom from the second Al monolayer (at $z \approx -2$ Å). Oscillatory interaction profiles have already been reported on the surface of metals between adatoms [9], however, no reports have been found for interdiffusion.

When the Pt approaches the surface one or two Al atoms are released from the surface which, however, immediately return back to the top layer. We show the enlarged animation of the active region during injection, which can be found at a web page [42]. It is more or less clear from this animation that the release of few Al atoms to the surface induces the injection of Pt. Finally, the injection of the Pt goes together with the ejection of an Al adatom and the Pt atom is captured below the top layer. Prior to the injection we can see a specific mechanism. Two or three Al atoms are released ballistically towards the approaching Pt atom and return back to the surface in less than 0.1 ps (this Al atom "receives" the host atom). The maximum vertical amplitude of the transient Al atoms can reach ~ 2 Å. This ultrafast out-of-plane vibration of the surface Al atoms do not lead to injection yet. Typical This strongly anharmonic behavior of the Al surface is shown in the upper panel of Fig. 2 where the trajectories of the transient vertical jump of few Al atoms to the surface (adlayer) can be seen. The sharp potential energy wells in lower panel of Fig. 1 also occur due to the transient out-of-plane processes.

Haftel *et al.* reported an unconventional exchange mechanism for Au/Ag(111) diffusion process involving multiple substrate atoms which catalyze interdiffusion [19]. They used, however, a reversed annealing simulation technique which speeds up atomic jumps. Nevertheless, they could conclude that the activation energy of this specific mechanism is very low. Moreover a collective double exchange process has been found which can be activated ballistically by an incoming deposited atom. These features are very similar to that found for the Pt/Al system. However, we repeated the simulation for Au/Ag(111) (without reversed annealing) at nearly 0 K using the same simulation conditions outlined for Pt/Al, and found no injection of Au to Ag(111). Also, at elevated temperatures (simulations have been carried out up to 300 K) the system does not show up any interdiffusive behaviors up to few picoseconds (not even on a longer time scale). However, if we set $r_0 < 2.8$ Å (if we take the elemental average, $r_0 = 2.9$ Å), Au does intermix to the Ag(111) topmost layer within 2 ps.

Hence few diffusion couples are only available until now, including Pt/Cu [20] and the Pt/Al(111) (also Ir,Au/Al(111)) systems presented in this work which show apparent anomalous intermixing behavior. Few other systems, such as the Au/Ag(111) couple could be the subject of a classification of anomalously interdiffusing systems. Under the effect of forced conditions, such as the low-energy ion-sputtering of the Pt/Ti interface we also find super-interdiffusion (ballistic jumps) of Pt in the Ti substrate and also the nonlinear scaling of $\langle R^2 \rangle$

has been obtained from simulations [16]. The anomalous nature of interdiffusion in Pt/Ti has also been confirmed by Auger electron spectroscopy depth profiling as a well-defined long range tail in the concentration profile of Pt [16]. This finding provides further evidence for the anomalous mass transport behavior of Pt in various media. In most of the diffusion couples with no interfacial anisotropy (atomic mass and size isotropy) no anomalous features have been found [16] and vanishingly small intermixing length have been measured and calculated [22]. However, we do believe that anomalous intermixing and impurity caused disordering of the surface of various solids are more widespread in nature than previously thought. In order to understand the details of the anomalous atomic transport we study the motion of atoms following their trajectories during the deposition events.

A. Atomic trajectories in the upper layers

In order to understand more deeply the mechanism of atomic injection of Pt, we plot the atomic positions of a crosssectional slab cut in the middle of the simulation cell (with a slab thickness of 15 Å) for the top layer atoms during vapor deposition of Pt with the average $r_0 \approx 2.8$ Å of the elemental values (upper Fig 2) at 0 K. The out-of-plane movement of Al atoms is rather strong during injection, while no such movements (or with only much smaller amplitude) can be seen when injection is suppressed by setting $r_0 = 3.1$ Å (the lower panel of Fig 2). We conclude that the presence of the impurity atom is necessary for disordering the surface layer locally.

The positions of the energetic atoms are also shown at ~ 0 K simulation in Fig 2. We can see a chaotic dynamics and in certain cases turbulent or circulating atomic motions around the equilibrium lattice sites. In certain cases the circulating atomic trajectories could also be characterized by vortices (see the enlarged image of the pattern in the right inset of the upper panel of Fig 3). The turbulent movement of atoms leads to large lateral and out-of-plane amplitudes of atomic vibrations.

We see no such state of surface atoms in the pure Al simulation cell nor in the cases when r_0 is set to above a critical value ($r_c > 3.1$ Å). The presence of a Pt atom is necessary for the emergence of the surface disordered matter. Moreover, the onset of the disordered atomic motions seem to be a necessary condition of injection of Pt atoms (this will be shown in subsection C). The injection of Pt requires the collective motion of few vibrating surface atoms. The assistance of at least two transient substrate adatoms with large vertical amplitudes seems to be a necessary condition for the injective mechanism.

In the upper panel of the left inset Fig 2 the top view of the atomic trajectories of a central vibrating atom is shown surrounded by 6 other atoms which suggests that the injection of Pt requires the collective motion of few vibrating surface Al atoms with a hexagonal sym-

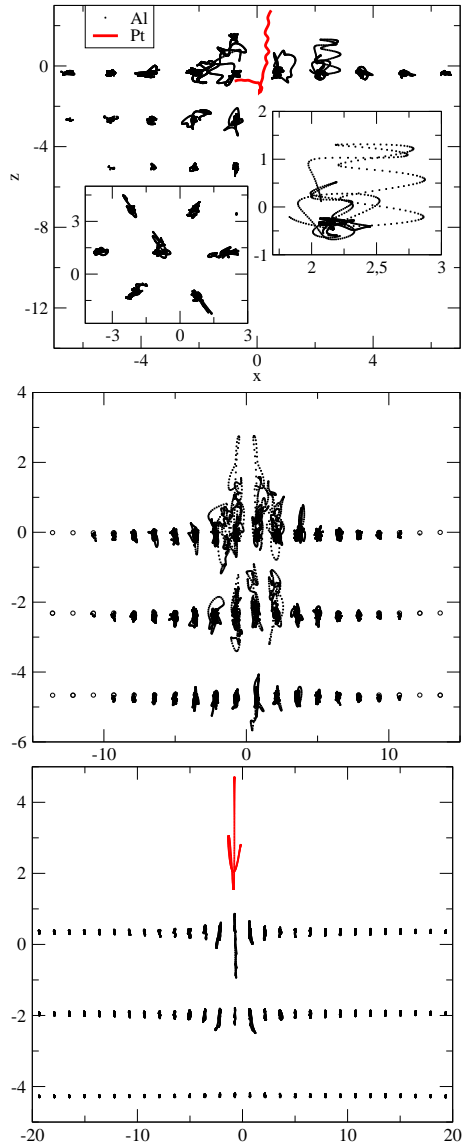


FIG. 2. The crosssectional view of typical trajectories of surface Al atoms induced by the deposition of a Pt atom at 0 K (the xz cut of the simulation cell, the scale is in Å in the axes). The positions of the Al atoms are collected up to 1 ps. The first neighbor distance $r_0 = 2.8$ Å. *Inset on the right:* The enlargement of a typical pattern of atomic dynamics of a surface Al atom as a crosssectional view. *Inset on the left:* Top view (seen from the (111) surface) of lateral atomic trajectories in the central region of the surface in the top layer. The displaced Al atoms are arranged in a hexagonal lattice. *Middle Figure:* Chaotic trajectories obtained under the same conditions given above except that the first neighbor distance r_0 is set to 2.5 Å. Initial atomic positions are also shown with larger filled circles. *Lower Figure:* Atomic trajectories obtained for $r_0 = 3.1$ Å

metry. Interestingly the lateral motion of these atoms is anisotropic: the atoms follow an elongated nearly one-dimensional trajectories. Another atoms surrounding the 7 "active" Al atoms are much less affected by the impurity atom, and the 2nd neighbors are nearly unperturbed lattice atoms on the surface. Hence, we can say, that when injection occurs atomic vibrations should be coupled with each other in order to open up a channel (an empty surface site) for Pt.

Tuning r_0 we also observe the onset of chaotic atomic trajectories. In the middle panel of Fig. 2 it can be seen that the atomic motions become extremely chaotic when $r_0 \leq 2.5$ Å. Further decrease in r_0 give rise to the ejection of a pair of Al atoms to the vacuum. This kind of an approach raises the question whether at least a partly chaos assisted mechanism could be responsible for the anomalous atomic transport. The analysis of the Lyapunov exponent (that is the measure of the chaotic processes) of the system [40] could give the answer for this question. Preliminary results indeed indicates that the presence of the surface impurity induces atomistic chaos on the surface of Al(111) [59]. These results will be published elsewhere.

The local disordered surface state persists until nearly less than a ps. Also, we find the ejection of an Al atom towards the vacuum (becomes a sputtered atom) when the EA EAM potential is used. Hence, there are similarities and differences between the CR and EAM potentials. Using the CR potential we find no sputtered Al atoms and usually a single Al atom is ejected to the surface while with the EA Al and Johnson's cross EAM potential 2-4 atoms or more are ejected to the surface and one of them is released to the vacuum. Using either the simple average of the elemental potentials as a heteronuclear potential or the crosspotential obtained by the Johnson's scheme [55] we also find injection with the EA EAM potential. Hence, the injective superdiffusion of Pt is not the specific artificial feature of the CR potential but is rather a generic feature of the EAM-model. The validity of the predicted superdiffusive features should be checked by more sophisticated *ab initio* MD approach. This could be an apparent work to be done in the future. Although, *ab initio* calculations can be carried out for a substrate with the number of atoms up to ~ 100 with present day supercomputers, therefore the obtained results could also be treated with care.

B. Acceleration towards the surface

The deposition of impurity atoms over the substrate surface leads to the local acceleration of the particle and to the impact to the surface with few eVs kinetic energy even if initiated by zero velocity. Hence the phenomenon of acceleration of the deposited impurity atom precedes the injection which has already been a well-known phenomenon [17,20,57,58]. Recently, Lee *et al.*

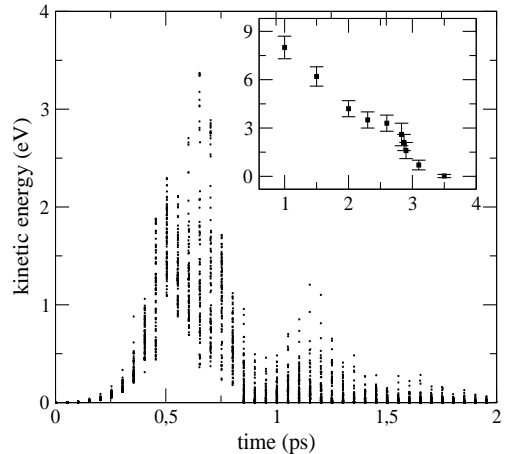


FIG. 3. The kinetic energy of the accelerating deposited particle as a function of the time (ps) using the Cleri-Rosato tight-binding potential ($r_0 = 2.83$ Å in the crosspotential al. The particle is initialized 4 Å above the free (111) surface of the Al with nearly zero velocity. The plotted points have been collected during few dozens of events with randomly varied impact points within the $(x, y) = +1; -1$ (Å) region of the surface. *Inset*: The peak kinetic energy of the accelerating deposited particle Pt before the impact to the surface (eV) as a function of the first neighbor distance (r_0) in the heteronuclear potential. The error bars denote standard deviations obtained for few simulation events at each of the r_0 points.

demonstrated that the low-energy deposition of Ni on Al(001) leads to serious acceleration of the Ni atoms striking the Al(001) surface with 3 – 4 eV kinetic energy [58]. In another study Wang *et al.* found the acceleration of Au particles over the Ag(110) surface. Moreover they also find the intermixing of the Au atoms with the Ag substrate in 11 % of the events in the first 6 ps of the simulations [17]. In the rest of the events the Au atoms remain above the surface. In certain cases acceleration of deposited particles leads to impact mixing (injection, e.g. in Pt/Cu) and it has been explained by the large negative heat of solution of this system [20]. Although this conclusion is based simply on the comparison of few diffusion couples which have different heat of solution. However, we demonstrate in this article that not heat of mixing (ΔH_m , or heat of solution) is the decisive factor of anomalous mixing.

We find that even if an artificially repulsive heteronuclear potential is used ($\xi = 0$ in Eq. (3)) impact mixing does occur for Pt/Al or Pt/Cu couples. Also, local acceleration does occur with a weakly attractive interaction when e.g. a noble gas Ar atom is deposited on Al (in this case no mixing occurs) with a peak kinetic energy of ~ 2 eV.

The acceleration of the deposited particle can be followed in Fig. 3 when the initial velocity is zero. The kinetic energy of the accelerating particle is given in eV

as a function of time using the CR potential (obtained for few tens of events) the peak value of ~ 3 eV is found when a Pt atom is deposited with zero initial velocity. The variation of the strength of the heteronuclear interaction in the potential (ΔH_m) does not affect the speed of acceleration and the peak values of the kinetic energy, e.g., if we set the preexponential $\xi = 10$. in Eq. (3), we set in a huge value of heat of mixing in the Al-Pt potential (and a very strong internuclear attraction with a very deep potential energy well in the potential), however, we find that the acceleration of Pt is not affected by the deeper potential well in the crosspotential. Also, if we set in smaller values, or even $\xi = 0$ could be set in (purely repulsive potential, only the Born-Mayer term is nonzero given in Eq. (4)), no change in acceleration is observed. Hence we conclude that the speed of acceleration is not affected by the strength of the Al-Pt potential and the generally accepted opinion, that the particle acceleration above solid surfaces is due to the large heat of solution of the corresponding alloy system, is not supported [20]. In other words we find that not the thermodynamic bias, built in the cross-interaction (via the depth of the potential well) drives the acceleration of the particle during deposition.

The variation of r_0 in the crosspotential does influence, however, the speed of acceleration. We find a correlation between r_0 and the peak kinetic energy of the particle (see inset upper Fig. 3). Although there is some scatter in the data, however, the trend is evident. Adjusting the size-mismatch the kinetic energy of the particle impact can be tuned by varying the relative positions of the minima of the potential wells (the ASM). At the average r_0 of the elemental values (~ 2.83 Å) the abrupt change of the kinetic energy can be seen which reports us that the system is increasingly sensitive to the variation of r_0 at the physically realistic values of ASM. Decreasing r_0 we find the amplification of surface instability and the enhancement of out-of-plane vibrations. The emergence of the injective mixing mechanism could be due to the ASM induced surface lattice instability (local impurity induced heating up the surface).

No acceleration of a standing particle is observed when the atom is initialized from above 6 Å the surface. We find the same decay distance of the surface long range forces when the cutoff distance of the crosspotential is increased above this value.

Depositing Al atom on Al(111) acceleration also occurs (self-atomic acceleration). The most of the deposition events with various host-substrate couples lead to accelerative deposition regardless to the chemical nature of the interacting couples.

The amplification of the out-of-plane vibration of Al atoms during deposition gives rise to the oscillation of the electronic density ρ of few surface atoms and to a long-range density tail above the surface. The long range forces (which initialize and speed up the acceleration) could be induced by the long range tail of the embedding function as a function of the density ρ in Eq. (2). Due

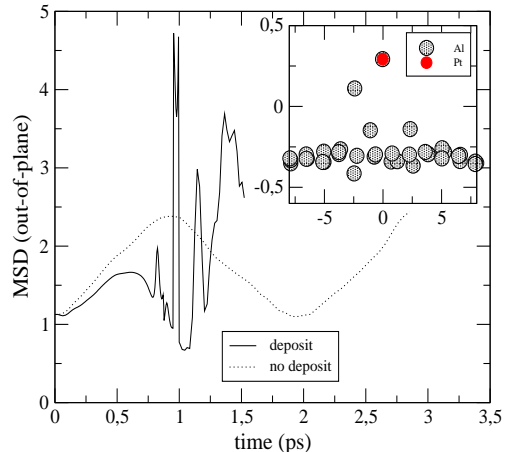


FIG. 4. The mean square of out-of-plane atomic displacements (MSD, $\langle R^2 \rangle_z$, Å²) of few Al atoms in the topmost layer in the injection zone (5×5 Å²) as a function of simulation time (ps) during deposition and without deposition (surface waving) using the Cleri-Rosato potential. The deposited atom is initialized 4.6 Å above the surface. *Inset*: The crosssectional view of the uppermost layer at $t = 0.95$ ps with the approaching Pt atom (together with the transient Al atoms).

to the out-of-plane instability of Al the electron density decays slowly above the surface and which gives rise to slowly damping $F(\rho)$. This could lead to the enhancement of the impurity-surface interaction.

C. The enhancement of surface disordering

In order to point out the correlation between the vibrational amplitude of the surface atoms and the acceleration of the deposited Pt atom we plot in Fig 4 the mean square of atomic out-of-plane displacements $\langle R^2 \rangle_z$ of few surface Al atoms in the middle of the simulation cell on the surface (using a 5×5 Å² area) as a function of the time (ps). In Fig 5 we plot the lateral $\langle R^2 \rangle_{xy}$ in order to demonstrate the enhancement of lateral movements of the surface Al atoms in the "active" region when the injection takes place. This, together with Fig 5 confirms that the abrupt activation of a surface disordering mechanism is necessary for the injection of the Pt atom. In Fig 4 the abrupt increase of $\langle R^2 \rangle_z$ at ~ 1 ps has been found which indicates the appearance of transient Al adatoms on the surface (see inset Fig 4). This transient process coincides with the injection of Pt and catalyzes intermixing in a similar way as proposed by Haftel *et al.* [19].

The injection of the impurity particle starts with the acceleration of the Pt atom. In turn the approaching particle induces the amplification of the out-of-plane vibration of few Al atoms which further accelerates the impurity particle towards the surface. Finally, at a critical proximity to the surface ($d_{PtAl} \leq 3$ Å) strong lateral

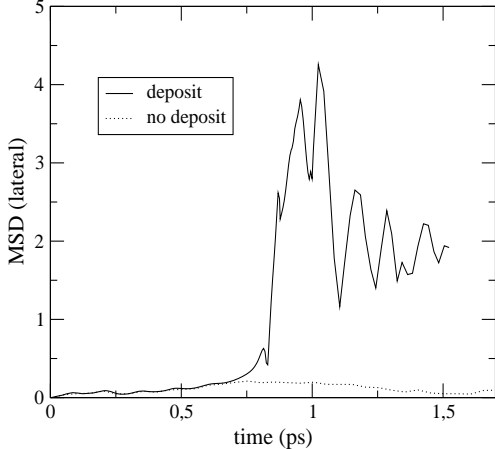


FIG. 5. The mean square of lateral atomic displacements ($\text{MSD}_{xy, \text{\AA}^2}$) of few Al atoms in the topmost layer in the injection zone ($5 \times 5 \text{\AA}^2$) as a function of simulation time (ps) during deposition and without deposition using the Cleri-Rosato potential. The deposited atom is initialized 4.6\AA above the surface.

components to the surface atomic displacements sets in (the appearance of the disordered surface state) together with the out-of-plane components and which leads to the injection of the particle. Without the surface instability no injection occurs, the particle becomes an adatom. The concerted motion of few surface atoms opens up a channel for injection.

The amplification of the out-of-plane vibration of Al atoms during deposition gives rise to the oscillation of the electronic density ρ of few surface atoms and to a long-range density tail above the surface. The long range forces (which initialize and speed up the acceleration) arise from the long range tail of the embedding function as a function of the density ρ in Eq. (2). Due to the out-of-plane instability of Al the electron density decays slowly above the surface and which gives rise to slowly damping $F(\rho)$. This could lead to the enhancement of the impurity-surface interaction.

Concerning the generalization of the superdiffusive features of intermixing in Pt/Al, we can say that injection occurs in many other transition metal/Al systems. However, in certain cases (e.g. Cu/Al) we find that the injection of the deposited particles appears after the deposition of dozens of atoms. In these cases, the slight decrease of r_0 leads also to ultrafast injection. We see similar features in the case of the Ni/Au system [42]. As already mentioned above, injection also takes place in the Pt/Cu system in a very similar way as in Pt/Al. It might be the case that Pt shows superdiffusive features even in more media (substrate). It is also interesting, what happens if we invert the systems, e.g. the deposition of Al on Pt leads to the lack of interdiffusion during the time scale we can reach. However, if we set $r_0 = 2.1 \text{\AA}$, the deposited Al atom can be forced to interdiffuse to the Pt

phase [42]. Above this value no injection occurs. It must also be noted that in general we find a transition from superdiffusion towards normal diffusion, e.g. when the first neighbor distance is tuned. Finally we should emphasize that the observed anomalous atomic transport processes and phenomena (injection with superdiffusion, surface assisted acceleration, oscillatory deposit-surface interaction, disordered surface matter) might not be the artifact of the employed interaction potentials nor the PARCAS code. The agreement with experimental vapor sputter deposition results [21,24] as well as the accurate parameterization of the employed Al many body potentials [15,43,52,54] and the straightforward usage of them for the anharmonic effects of Al [27,57] provide solid basis for sharing these results with the wider community.

An important question remains to be resolved is whether a specific state of matter is found or the size-mismatched host-impurity interaction induced surface disordering can be considered as a local low-temperature premelting phenomenon. Anyhow, the impurity induced low-temperature disordering of the surface layers including few dozens of atoms is an unexpected short lived local state of the surface and calls for further verifications. Although its lifetime is short (less than a ps), however, this localized spatial and temporal surface state occurs at each impact events. This state of matter resembles a cascade event, however, its appearance does not depend on the impact energy of the impurity particle.

V. CONCLUSIONS

In this paper we studied the deposition of Pt on Al(111). An oscillatory adsorbate-surface interaction and ultrafast injective inter-layer atomic transport of the deposited vapor atoms has been found for the Pt/Al couple using two different types of atomic interaction potentials. The soft landing of the deposit induces the disordering of the local region of the surface Al atoms. The disordered state persists up to ~ 0.5 ps which covers the transient out-of-plane vibration of few surface Al atoms. The anomalous inter-layer transport of the impurity atom to the substrate is assisted by the transient out-of-plane motion of few surface Al atoms. This collective exchange mechanism works even at very low temperatures slightly above 0 K and calls for experimental verification.

Contrary to the general belief that chemical and thermodynamic forces govern particle deposition and interdiffusion no effect of thermodynamic bias has been found on acceleration towards the substrate's surface and on intermixing of the deposited particle. Instead we point out the role of atomic size-mismatch (ASM) in particle acceleration and in superdiffusive features. In particular we find that intermixing can be tuned by a system parameter which can be given as the ratio of the atomic size parameter of the cross-interaction term to the substrate's lattice constant (the ASM). Moreover, the chaotic nature

of atomic trajectories as well as the lattice instability of the surface can also be tuned by ASM.

This work is supported by the OTKA grant F037710 from the Hungarian Academy of Sciences. We wish to thank to K. Nordlund, to P. Barna, G. Ódor, L. Vitos, T. Kovács, T. Tél and to M. Menyhárd for helpful discussions. The help of the NKFP project of 3A/071/2004 is also acknowledged. The work has been performed partly under the project HPC-EUROPA (RII3-CT-2003-506079) with the support of the European Community using the supercomputing facility at CINECA in Bologna.

-
- [1] V.A. Schukin, N. N. Ledentsov, D. Bimberg, *Epitaxy of Nanostructures*, Springer (2004).
- [2] D. L. Beke, Z. Erdélyi, Phys. Rev. **B73**, 035426 (2006).
- [3] T. Michely, J. Krug, *Island, Mounds and Atoms*, Springer (2004).
- [4] R. Metzler, J. Klafter, Phys. Rep., **339**, 1. (2000).
- [5] R. van Gastel, E. Somfai, W. van Saarloost, J. W. M. Frenken, Nature, **408**, 665 (2000), D. Brockmann, T. Giesel, Phys. Rev. Lett., **90**, 170601-1 (2003),
- [6] W. Luo, K. A. Fichthorn, Phys. Rev. **B72**, 115433 (2005).
- [7] H. L. Meyerheim, V. Stepanyuk, A. L. Klavsyuk, E. Soyka, J. Kirschner, Phys. Rev. **B72**, 113403 (2005),
- [8] C. Polop, *et al.*, Surf. Sci. **575**, 89 (2005).
- [9] J. Repp, *et al.*, Phys. Rev. Lett., **85**, 2981 (2000),
- [10] J. Tersoff, Phys. Rev. Lett. **74**, 434-437 (1995)
- [11] V. S. Stepanyuk, *et al.*, Phys. Rev. **B63**, 235406 (2001),
- [12] H. Bulou, J-P. Bucher, Phys. Rev. Lett. **96**, 076102 (2006).
- [13] T.-L. Chan, C. Z. Wang, M. Hupalo, M. C. Tringides, and K. M. Ho, Phys. Rev. Lett. **96**, 226102-1 (2006).
- [14] N. A. Levanov, *et al.*, Phys. Rev. **B61**, 2230 (2000).
- [15] P. Süle, Surf. Sci., **585**, 170 (2005).
- [16] P. Süle, M. Menyhárd, L. Kótis, J. Lábár, J. F. Egelhoff Jr., preprint at: <http://babbage.sissa.it/archive/cond-mat/0605566>.
- [17] R. Wang, K. A. Fichthorn, Phys. Rev. **B51**, 1957 (1995).
- [18] S. Rousset, S. Chiang, D. E. Fowler, D. D. Chambliss, Phys. Rev. Lett. **69**, 3200 (1992), M. I. Haftel, M. Rosen, T. Franklin, M. Hettermann, Phys. Rev. Lett. **72**, 1858 (1994).
- [19] M. I. Haftel, M. Rosen, Surf. Sci., **407**, 16 (1998),
- [20] J. A. Sprague and C. M. Gilmore, Thin Solid Films, **272**, 244 (1996).
- [21] J. D. R. Buchanan, *et al.*, Phys. Rev. **B66**, 104427 (2002).
- [22] P. Süle, M. Menyhárd, Phys. Rev., **B71**, 113413 (2005).
- [23] P. Süle, M. Menyhárd, K. Nordlund, Nucl Instr. and Meth. in Phys. Res., **B211**, 524 (2003), **B226**, 517 (2004).
- [24] Zs. Radi, P. B. Barna, Surf. and Coat. Techn., **100-101**, 90. (1998).
- [25] J. A. Rodrigue, M. Kuhn, Chem. Phys. Lett., **240**, 435 (1995).
- [26] A. Kovács, P. B. Barna and J. L. Lábár, Thin Solid Films, **433**, 78 (2003).
- [27] R. Zivieri, G. Santoro, V. Bortolani, Phys. Rev. **B59**, 15959 (1999).
- [28] A. N. Al-Rawi, A. Kara, T. S. Rahman, Phys. Rev. **B66**, 165439-1 (2002).
- [29] P. R. Okamoto, N. Q. Lam, L. E. Rehn, Solid State Phys. **52**, 1. (1999).
- [30] P. Jalali and M. Li, Phys. Rev. **B71**, 014206 (2005).
- [31] J. Dalmas, *et al.*, Phys. Rev. **B72**, 155424 (2005).
- [32] M. Li, W. L. Johnson, Phys. Rev. Lett., **70**, 120 (1993).
- [33] H. W. Sheng, *et al.*, Nature, **439**, 419 (2006).
- [34] Y. Qi, *et al.*, Phys. Rev. **B59**, 3527 (1999).
- [35] E. S. Park, D. H. Kim, Appl. Phys. Lett. **86**, 201912 (2005).
- [36] M. Forsblom, N. Sandberg, G. Grimvall, Phys. Rev. **B69**, 165106-1, (2004).
- [37] K. Nordlund, Comput. Mater. Sci, **3**, 448. (1995), K. Nordlund, *et al.*, Phys. Rev. **B57**, 7556 (1998).
- [38] K. Nordlund, *et al.*, Nucl. Instr. and Meth. **B206** 189 (2003), M. Ghaly, K. Nordlund, and R. S. Averback, Phil. Mag. A **79**, 795 (1999), C. G. Zimmermann, *et al.*, Phys. Rev. Lett. **83**, 1163 (1999).
- [39] M. P. Allen, D. J. Tildesley, *Computer Simulation of Liquids*, (Oxford Science Publications, Oxford 1989)
- [40] D. Frenkel, B. Smith, *Understanding Molecular Simulation*, Academic Press (2002).
- [41] H. J. C. Berendsen, *et al.*, J. Chem. Phys., **81**, 3684 (1984).
- [42] <http://www.mfa.kfki.hu/~sule/animations/ptonal.htm>.
- [43] F. Cleri, G. Mazzone and V. Rosato, Phys. Rev. **B47**, 14541 (1993).
- [44] N. I. Papanicolau, H. Chamati, G. A. Evangelakis, D. A. Papaconstantopoulos, Comput. Mater. Sci., **27**, 191 (2003).
- [45] G. X. Li, C. S. Liu, and Z. G. Zhu, Phys. Rev. **B71**, 094209 (2005).
- [46] M. M. G. Alemany, O. Diguez, C. Rey, and L. J. Gallego, Phys. Rev. **B60**, 9208 (1999).
- [47] J.-W. Kang and H.-J. Hwang Phys. Rev. **B64**, 014108 (2001).
- [48] M. Folies, *et al.*, Phys. Rev. **B33**, 7983 (1986).
- [49] H. Rafi-Tabar, A. P. Sutton, Pilos. Mag. Lett., **63**, 217 (1991), W. Eckstein, *Computer Simulation of Ion-Solid Interactions*, Springer, Berlin (1991).
- [50] C. Goyhenex, *et al.*, Phys. Rev. **B60**, 2781 (1999).
- [51] H. de Waal, R. Pretorius, Nucl Instr. and Meth. in Phys. Res., **B158**, 717 (1999).
- [52] M. S. Daw, S. M. Foiles, M. I. Baskes, Mat. Sci. and Engr. Rep., **9**, 251 (1993).
- [53] M. I. Haftel, M. Rosen, Phys. Rev. **B51**, 4426 (1995).
- [54] F. Ercolessi, J. B. Adams, Europhys. Lett., **26**, 583 (1994).
- [55] R. A. Johnson, *et al.*, Phys. Rev. **B39**, 12554 (1989).
- [56] C. Busse, C. Engin, H. Hansen, U. Linke, T. Michely, H. M. Urbassek, Surf. Sci., **488**, 346 (2001).
- [57] M. Villarba and H. Johnsson, Phys. Rev. **B49**, 2208 (1994).
- [58] K-R. Lee, *et al.*, J. Mag. and Mag. Mat., **286**, 394 (2005).
- [59] P. Süle, T. Tél, unpublished results.
- [60] M. Atakhorrami, *et al.*, Phys. Rev. Lett. **95**, 208302 (2005), C. R. Nugent, W. N. Quarles, T. H. Solomon, Phys. Rev. Lett. **93**, 218301 (2004).